Photophysics of *Fac*-Tris(2-Phenylpyridine) Iridium(III) Cored Electroluminescent Dendrimers in Solution and Films

Ebinazar B. Namdas, Arvydas Ruseckas, and Ifor D. W. Samuel*

Organic Semiconductor Centre, School of Physics and Astronomy, University of St. Andrews, North Haugh, St. Andrews, Fife, KY16 9SS, United Kingdom

Shih-Chun Lo and Paul L. Burn*

The Dyson Perrins Laboratory, University of Oxford, South Parks Road, OX1 3QY, Oxford, United Kingdom

Received: June 11, 2003; In Final Form: November 6, 2003

We present time-resolved photoluminescence (PL) studies of novel first- and second-generation electrophosphorescent *fac*-tris(2-phenylpyridine) iridium(III) [$Ir(ppy)_3$] cored dendrimers and compare them with neat films of molecular $Ir(ppy)_3$. A PL quantum yield of ~0.8 is observed in blends of the dendrimers with 4,4′-bis(*N*-carbazolyl)biphenyl (CBP) at room temperature, and the natural radiative lifetime of the emissive state (1.5 μs) is observed to be the same for dendrimers and molecular $Ir(ppy)_3$. Quenching of the PL occurs in neat films, because of an energy transfer to less-emissive sites, which have ~10 times lower oscillator strength. The PL quenching rate in spin-coated films of the first- and second-generation dendrimers is slower by a factor of 11 and 20, respectively, as compared to neat $Ir(ppy)_3$ films prepared by evaporation. Dendrimer films showed a much smoother surface than $Ir(ppy)_3$ films, which is consistent with more extensive aggregation of molecular $Ir(ppy)_3$ than dendrimers.

1. Introduction

Organic light-emitting diodes (OLEDs) are currently under intense investigation for application in the next generation of flat-panel-display technologies. Over the past few years, much progress has been made in electroluminescence, because of the continuing discovery of new and improved materials. Light-emitting materials for these devices can be divided into three classes: small organic molecules that are usually evaporated,[1] solution-processed conjugated polymers,[2−4] and more recently solution-processed dendrimers.[5−10] The majority of OLEDs reported to date emit light by fluorescence. Recently, *fac*-tris-(2-phenylpyridine) iridium(III) [$Ir(ppy)_3$] and related iridium-(III) complexes have received attention as efficient phosphorescent emitters.[11−13] These complexes are very attractive for display applications, because they can harvest both singlets and triplets and, hence, give 100% internal quantum efficiency.[11] Further advantages of these materials are that the emission color can be tuned by changing the chemical structure of the ligands, and the short triplet lifetime of ~1 μs reduces luminescence quenching, because of excitation transfer to quenching sites and triplet−triplet annihilation. $Ir(ppy)_3$ shows intense phosphorescence in solution at room temperature with the photoluminescence quantum yield (PLQY) in solution, which is reported to be 0.5 ± 0.2.[14,15] However, despite numerous studies on Ir-$(ppy)_3$, we are not aware of its PLQY value being reported for neat films.

Films that contain $Ir(ppy)_3$ are generally made by evaporation under high vacuum. Solution processing techniques such as spin-coating or inkjet printing can lead to simpler fabrication of devices. Therefore, we have pursued the development of highly luminescent solution-processible electrophosphorescent dendrimers.[5,6] Dendrimers are macromolecules that are comprised of three components: a central core, dendrons (branches), and surface groups that are located at the distal ends of the dendrons. Dendritic structures allow the control of intermolecular interactions between phosphorescent emitters; thus, they make it possible to tune the charge-transporting properties independently from light emission. Green light-emitting dendrimers with Ir-$(ppy)_3$ as their core have been used to make the most-efficient OLEDs with a solution-processed light-emitting layer reported to date.[5,6] Photophysical studies of the $Ir(ppy)_3$ chromophore in dendritic structures provide information on the dynamics of excited states, which are also formed in OLEDs from injected electrons and holes, and can help to design materials with improved properties.

In this paper, we compare the photoluminescence (PL) dynamics of $Ir(ppy)_3$-cored dendrimers with the simple molecule $Ir(ppy)_3$ in solution, blends, and neat films. In solution and blends, these dendrimers are characterized by high PLQY values and a PL lifetime of 1.2 μs, whereas neat films show lower PLQY values, faster PL decay, and the appearance of a red-shifted luminescence band at >1 μs after photoexcitation. The increase of the spacing between $Ir(ppy)_3$ moieties in dendrimer films substantially decreases the PL quenching rate. This observation correlates with the much smoother surface of dendrimer films, as shown by atomic force microscopy (AFM), which indicates the absence of aggregation, in contrast to that observed with $Ir(ppy)_3$ films.

2. Experimental Section

The chemical structures of the $Ir(ppy)_3$, and the two dendrimers used in this study, are shown in Figure 1. The first-generation (Ir-G1) and second-generation (Ir-G2) dendrimers

* Authors to whom correspondence should be addressed. E-mail addresses: idws@st-andrews.ac.uk, paul.burn@chem.ox.ac.uk.

10.1021/jp035664k CCC: $27.50
Published on Web 01/10/2004

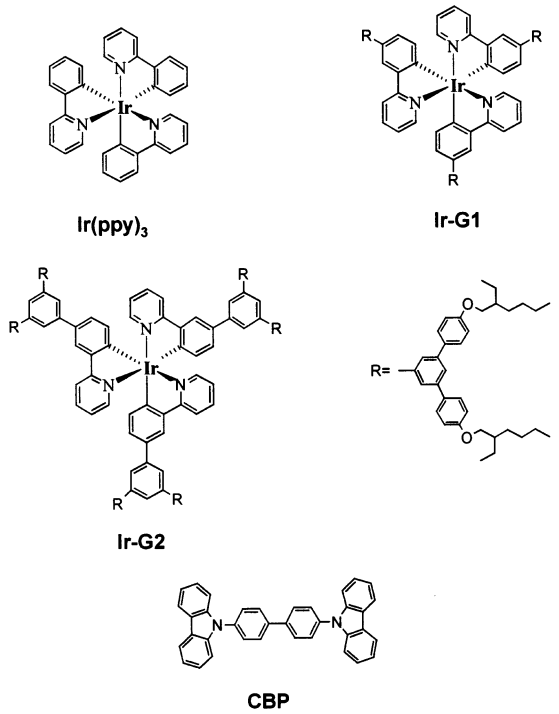

Figure 1. Molecular structure of *fac*-Ir(ppy)$_3$, first-generation Ir-G1, second-generation Ir-G2, and 4,4′-bis(*N*-carbazolyl)biphenyl (CBP).

contain an Ir(ppy)$_3$ core, phenylene-based dendrons, and 2-ethylhexyloxy surface groups. Solutions were made using high-performance liquid chromatography (HPLC)-grade solvents and were degassed by three freeze−pump−thaw cycles before measurements. Dendrimer films were made by spin-coating from a chloroform solution onto fused silica substrates at typical concentrations of 10 mg/mL and a spin speed of 800 rpm. Ir(ppy)$_3$ films were deposited by evaporation at a pressure of $\sim 10^{-6}$ Torr and a rate of 0.1−0.5 nm/s. Ir(ppy)$_3$ is commonly used in a blend with 4,4′-bis(*N*-carbazolyl)biphenyl (CBP), and 7 wt % Ir(ppy)$_3$:CBP blend films were made by the coevaporation of Ir(ppy)$_3$ and CBP. The thickness of the evaporated layers was monitored by an in situ quartz crystal microbalance that had been calibrated using a Dektak^3 surface profilometer.

PL kinetics were measured using the time-correlated single-photon-counting technique. Excitation occurred at a wavelength of 390 or 500 nm by pulsed light-emitting diodes (Picoquant, model PLS 370). The excitation light of 10 pJ/pulse at a pulse repetition rate of 100 kHz was focused onto a spot 0.5 mm in diameter. The emitted light was dispersed in a monochromator with an entrance slit that corresponded to a bandwidth of 8 nm and was detected with a cooled microchannel plate photomultiplier tube (Hamamatsu, model RU-3809U-50). The apparatus response function was ∼350 ps (full width at half maximum, fwhm) on its fastest scale. Time-resolved PL spectra were measured in a time window of 0−5 μs with a Hamamatsu streak camera, using 100-fs pulses for excitation at 400 nm and a pulse repetition rate of 5 kHz. All measurements were performed at room temperature. Films were kept in a vacuum of $<10^{-3}$ mbar during time-resolved PL measurements. The decay kinetics were fitted by a sum of exponential functions: $I(t) = A_1 \exp(-t/\tau_1) + A_2 \exp(-t/\tau_2) + A_3 \exp(-t/\tau_3)$, where the A and τ terms represent the pre-exponential factors and time constants, respectively. The quality of the fits was confirmed by random distribution of the residuals. The average lifetimes were calculated as $\langle\tau\rangle = \sum_i(A_i\tau_i)/\sum_i A_i$.

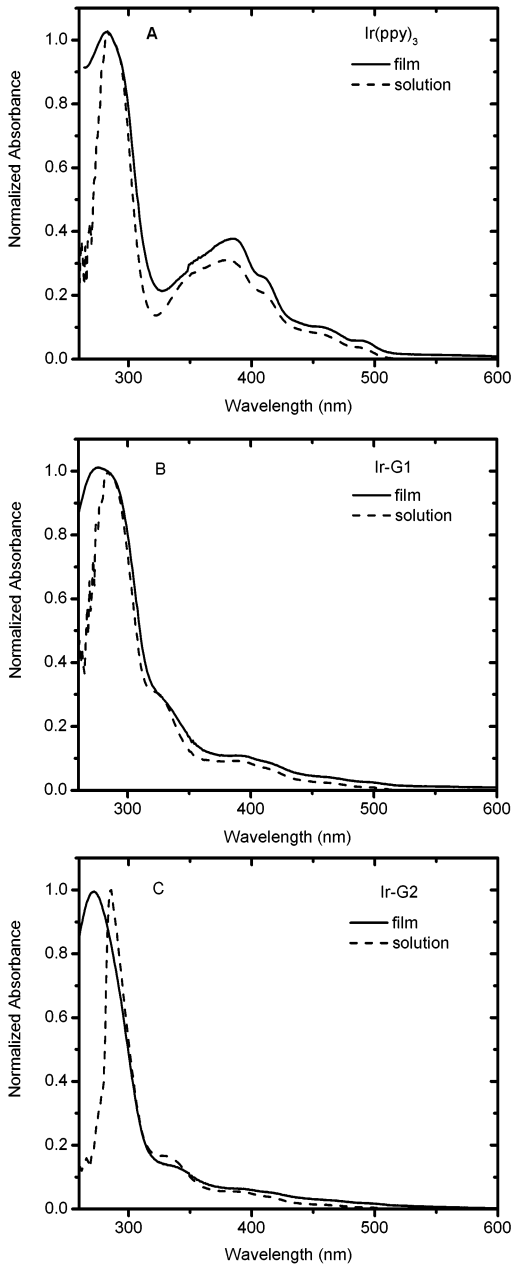

Figure 2. Normalized ground-state absorption spectra of (A) Ir(ppy)$_3$, (B) Ir-G1, and (C) Ir-G2 ((− − −) in solution and (—) neat film).

Absorption spectra were recorded on a Cary Varian model 300 absorption spectrophotometer, and time-integrated PL spectra were measured on a Jobin Yvon Fluoromax 2 fluorimeter. The solution PLQY value was measured by a relative method, using quinine sulfate in 0.5 M sulfuric acid, which has a PLQY value of 0.51 as the standard.[16] The samples were excited at a wavelength of 360 nm, and the optical densities of the standard and the samples were similar and small (∼0.1). The PLQY of the solid films was measured in an integrating sphere under a flowing nitrogen atmosphere, in accordance with Greenham et al.,[17] using a helium−cadmium laser with a wavelength of 325 nm and an excitation power of ∼0.2 mW.

3. Results and Discussion

A. Steady-State Absorption. The absorption spectra of Ir(ppy)$_3$ (Figure 2A) in solution (dashed line) and in film (solid lines) show an intense band in the range of 250−320 nm, which

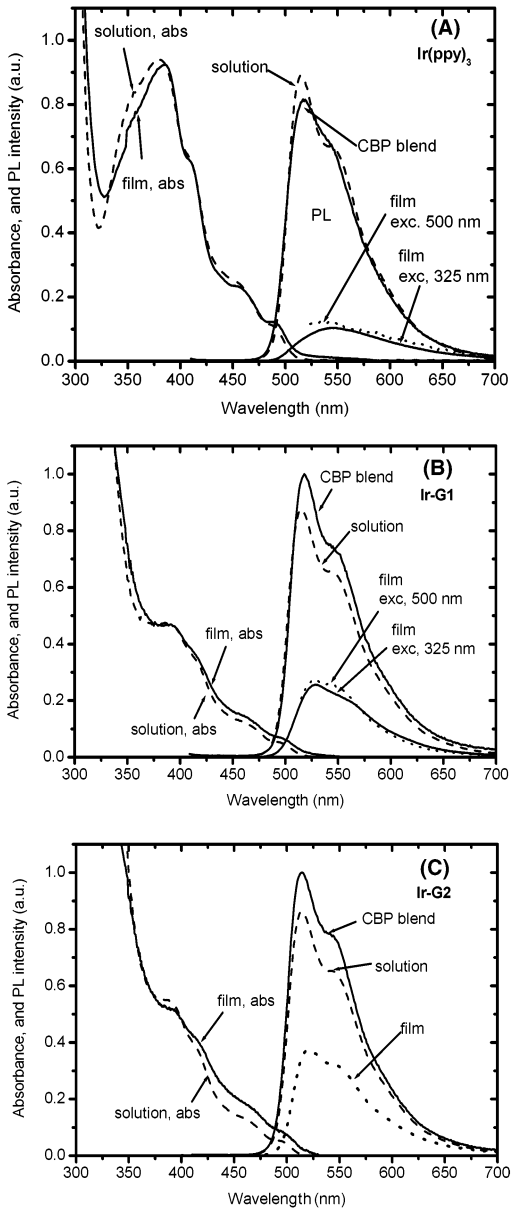

Figure 3. Absorption and steady-state photoluminescence (PL) spectra of (A) $Ir(ppy)_3$ in degassed toluene solution, evaporated neat $Ir(ppy)_3$ film, and 7 wt % $Ir(ppy)_3$:CBP blend; (B) Ir-G1 in toluene solution and film; and (C) Ir-G2 in toluene solution and film. PL spectra are scaled according to the measured PLQY values.

is due to the singlet−singlet $\pi-\pi^*$ transitions of the ligand.[13,14] A weaker absorption band extends from 330 nm to 500 nm, where calculations have predicted several singlet−singlet metal-to-ligand charge transfer (MLCT) transitions,[18] the lowest of them at 2.8 eV (443 nm). The relative intensity of the 250−320 nm band in Ir-G1 is approximately twice as large as that in $Ir(ppy)_3$, because of an additional contribution to the absorption from the biphenylene-based dendrons. A further increase of the UV absorption band is observed in Ir-G2, because of the increase in the number of biphenylene units. The absorption spectra of thin films are similar to dilute solutions, except that the UV band is broader, which can be explained by inhomogeneous broadening that is due to conformational disorder of the dendrons in films.

B. Photoluminescence in Solution and Blends. The time-integrated PL spectra of $Ir(ppy)_3$ and the two dendrimers in dilute solution and blends (Figure 3) are almost identical. There is very little overlap between the absorption and emission

TABLE 1: Position of PL Maximum (λ_{em}^{max}), Photoluminescence Quantum Yield (PLQY), Phosphorescence Lifetime (τ_{Ph}), Radiative Lifetime (τ_R), and Nonradiative Lifetime (τ_{NR}) of $Ir(ppy)_3$ and Dendrimers in Solution and Blends

sample	λ_{em}^{max} (nm)	PLQY[a]	τ_{Ph} (μs)[b]	τ_R (μs)	τ_{NR} (μs)
Ir-G1 film					
Ir-G1 in toluene	515	0.70	1.0[c]	1.5	3
20 wt % Ir-G1 in CBP	518	0.80	1.2	1.5	6
Ir-G2 film					
Ir-G2 in toluene	515	0.69	1.0[c]	1.5	3
20 wt % Ir-G2 in CBP	515	0.80	1.2	1.5	6
$Ir(ppy)_3$ film					
$Ir(ppy)_3$ in toluene, degassed	515	0.70	1.0[c]	1.5	3
$Ir(ppy)_3$ in toluene, nondegassed	515	0.02	0.032	∼1.6	0.033
7 wt % $Ir(ppy)_3$ in CBP	518	∼0.5	0.7[c]	∼1.4	∼1.4

[a] Uncertainty is ±10% of the measured value. [b] Uncertainty is ±5%. [c] Average lifetime of the two-exponential decay.

spectra. The PLQY value of $Ir(ppy)_3$ was 0.7 ± 0.07 in degassed toluene, which is close to the value of 0.50 ± 0.20 that has been reported in the literature.[15] The PLQY value of $Ir(ppy)_3$ in nondegassed toluene solution is quenched substantially to 0.03, which indicates that the removal of dissolved oxygen is crucial for accurate measurements of PLQY. The PLQY values of Ir-G1 and Ir-G2 are 0.70 ± 0.07 and 0.69 ± 0.07, respectively. Similar to $Ir(ppy)_3$, the dendrimer samples are sensitive to dissolved oxygen and the luminescence is quenched substantially in nondegassed solution. PLQY values of 0.8 ± 0.08 are obtained for the blends of 20 wt % Ir-G1 and Ir-G2 dendrimers in CBP (Table 1).

The PL decay kinetics for $Ir(ppy)_3$, Ir-G1, and Ir-G2 are shown in Figure 4. In degassed solutions, the decay kinetics of all three materials are independent of the detection wavelength in the range of 500−600 nm and dominated by a long 1.2-μs component. The PL lifetime in the nondegassed solution decreases dramatically to ∼30 ns. The long lifetime of the PL and quenching by oxygen are signatures of phosphorescence. We, therefore, can safely assign the green emission with a maximum at 515 nm to the radiative decay of the triplet state ^{3}(MLCT) to the ground state. The peaks at 515, 555, and ∼600 nm are equally spaced by ∼1400 cm^{-1} and attributed to the 0−0, 0−1, and 0−2 vibronic transitions, respectively. The 0−0 transition at 515 nm is slightly lower in energy than the calculated vertical transition energy of MLCT (at 2.59 eV, 479 nm) between the lowest triplet state and the ground state,[18] which can be explained by structural relaxation in excited state and solvation. PL decays in solution also show a short component of ∼0.15 μs with a relative amplitude of ∼0.15, which could be due to the presence of the meridional isomer or the increase of the nonradiative deactivation rate in some molecules by formation of the excited-state complex with residual oxygen. The meridional isomer has been shown to have a similar PL spectrum to the facial isomer but much faster nonradiative decay, which could be due to the conformational changes in the excited state.[19] In blends of Ir-G1 and Ir-G2 at 20 wt % in CBP, the PL decay is monoexponential, with a lifetime of 1.2 μs. The absence of the fast-decay component, in contrast to solution, may be due to reduced conformational freedom of the molecule in solid blends. The fast-decay component of 0.12 μs, with a relative amplitude of 0.3, is still observed in the 7 wt % $Ir(ppy)_3$:CBP blend, along with a dominant 1.2-μs component (with a relative amplitude of 0.7).

When only one type of emitting species is present in the sample, the phosphorescence lifetime (τ_{Ph}) and PLQY value are related to the radiative lifetime (τ_R) and the nonradiative lifetime

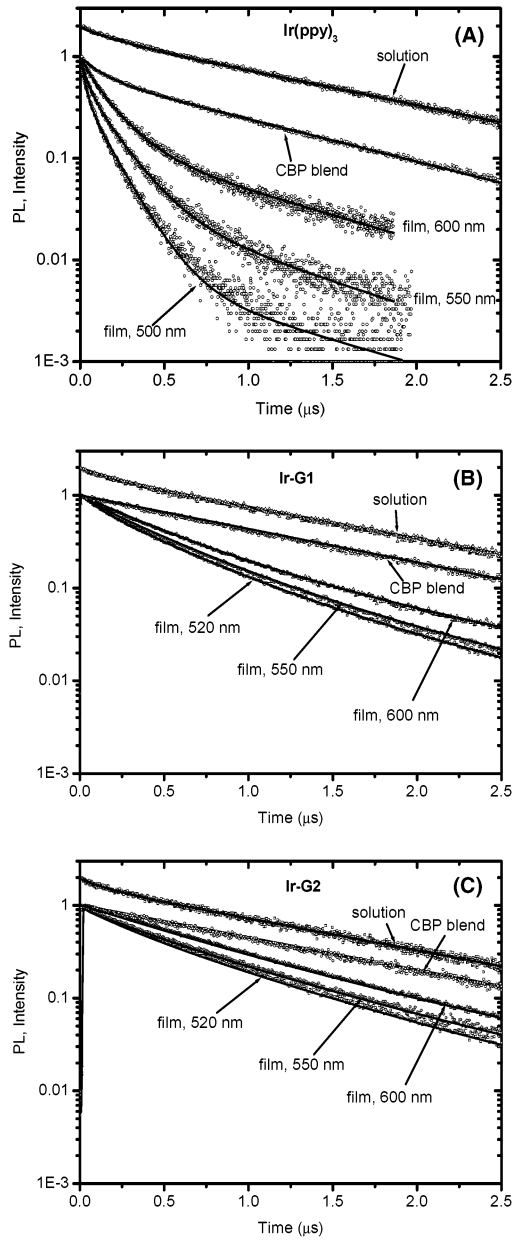

Figure 4. PL kinetics of (A) $Ir(ppy)_3$ in degassed toluene solution, evaporated neat $Ir(ppy)_3$ film, and 7 wt % Ir(ppy):CBP blend at various detection wavelengths; (B) Ir-G1 in degassed toluene solution, neat film, and 20 wt % Ir-G1:CBP blend at various detection wavelengths; (C) Ir-G2 in degassed toluene solution, neat film, and 20 wt % Ir-G2: CBP blend at various detection wavelengths. Solid lines are fits to a sum of exponential decays with the parameters given in Tables 1 and 2. PL kinetics of solution and CBP blend films were independent of detection wavelength in the range of 510−600 nm. Samples were excited at 390 nm, the decays are normalized, and, for clarity, solution decays are offset vertically.

(τ_{NR}) of the emissive state as

$$\frac{1}{\tau_{Ph}} = \frac{1}{\tau_R} + \frac{1}{\tau_{NR}} \quad (1)$$

and

$$PLQY = \eta\left(\frac{\tau_{Ph}}{\tau_R}\right) \quad (2)$$

where η is the quantum efficiency of the population of the emissive state from absorbed photons. Because no emission from the singlet state is observed, we assume η to be 1 and get $\tau_R = 1.5 \pm 0.2$ μs and $\tau_{NR} = 6 \pm 1$ μs for the Ir-G1 and Ir-G2 in the blends. The meridional isomer has been shown to have a τ_R value that is similar to that of the facial isomer;[19] therefore, we can use the average value of τ_{Ph} for solutions of $Ir(ppy)_3$, Ir-G1, and Ir-G2 in eq 2, giving a value of $\tau_R = 1.5 \pm 0.2$ μs that is identical for all samples (see Table 1). This indicates that addition of the dendrons to $Ir(ppy)_3$ does not change the luminescence properties of the $Ir(ppy)_3$ moiety in solutions and inert blends.

TABLE 2: Summary of Photoluminescence Data for Neat Films[a]

wavelength (nm)							
excitation	detection	τ_1 (μs)[b]	A_1[b]	τ_2 (μs)[b]	A_2[b]	τ_3 (μs)[b]	A_3[b]
	$Ir(ppy)_3$ film, $\lambda_{em}^{max} = 546$ nm, PLQY ≈ 0.12						
390	500	0.03	0.54	0.14	0.45	0.9	0.01
390	550	0.04	0.38	0.16	0.58	0.9	0.04
390	600	0.04	0.10	0.15	0.75	0.9	0.15
500	600	0.06	0.29	0.19	0.60	1	0.11
	Ir-G1 film, $\lambda_{em}^{max} = 528$ nm, PLQY > 0.22						
390	520	0.08	0.04	0.37	0.44	0.8	0.52
390	550	0.08	0.02	0.39	0.44	0.9	0.54
390	600			0.43	0.40	1	0.60
500	600			0.3	0.27	1	0.73
	Ir-G2 film, $\lambda_{em}^{max} = 521$ nm, PLQY > 0.31						
390	520			0.27	0.15	0.9	0.85
390	550			0.32	0.14	0.9	0.86
390	600			0.52	0.25	1	0.75

[a] The variable λ_{em}^{max} represents the maximum position in the time-integrated PL spectrum; PLQY values have been measured in the integrating sphere. Time constants and pre-exponential factors of a three-exponential decay have been fitted to the PL kinetics at different excitation and detection wavelengths. [b] Uncertainty in time constant τ and pre-exponential factor A is ±10%.

C. Photoluminescence of Neat Films. The PL spectrum of the neat $Ir(ppy)_3$ film prepared by evaporation (see Figure 3) is broad, and its maximum is substantially red-shifted (by 18 nm), in comparison to the solution and the blend with CBP. The shape of the PL spectrum is independent of the excitation wavelength in the range of 325−500 nm. The PLQY value is only ~0.12 in neat $Ir(ppy)_3$ film, which is much lower than that in solution and the blend, implying that intermolecular interactions are responsible for the quenching and the red shift of the PL spectrum in neat $Ir(ppy)_3$ films. The PL maximum position in neat films of Ir-G1 is only slightly red-shifted (by ~7 nm), in comparison to the blend of the same material with CBP, and the PL spectrum of Ir-G2 is basically the same as that in the neat film, blend, and solution. PLQY values of 0.22 and 0.31 were measured for neat films of the first- and second-generation dendrimers, respectively.

The PL decay in evaporated $Ir(ppy)_3$ film (Figure 4A) is much faster than that in solution and the blend, which indicates that additional nonradiative decay channels of the emissive triplet state prevail in the neat film. The parameters of the three-exponential decay function fitted to the measured PL kinetics are given in Table 2. The time constants of the fits—$\tau \approx 0.04$, 0.15, and 0.9 μs—are very similar for all detection wavelengths, only the relative amplitude of the long component increases as the detection wavelength increases. The average PL lifetime at 550 nm is 0.14 μs, which is similar to the reported value of ~0.10 μs in the literature.[20] The PL decay in neat films of dendrimers (panels B and C in Figure 4) is slower than in the $Ir(ppy)_3$ film, which is consistent with the higher PLQY in dendrimer films; however, it is still faster than that in solution

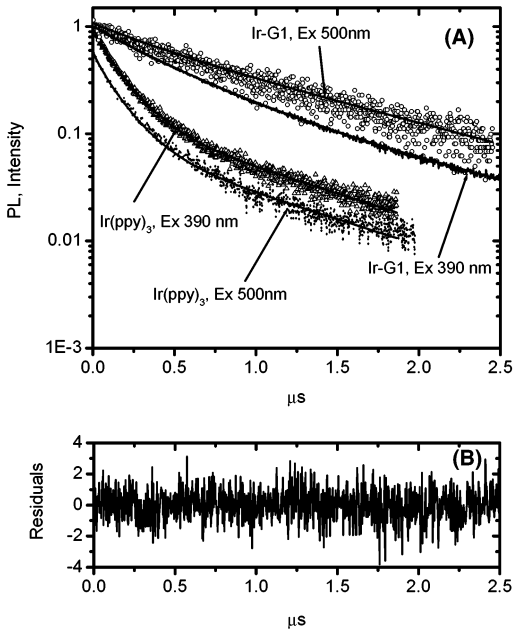

Figure 5. (A) PL kinetics of Ir-G1 neat film and $Ir(ppy)_3$ film at excitation wavelengths of 390 and 500 nm, respectively, and a detection wavelength of 600 nm. For clarity, the decay in $Ir(ppy)_3$ film at 390 nm excitation is offset vertically. (B) Residuals of the fit for a neat Ir-G1 film at an excitation of 390 nm.

and the blend, indicating that quenching of the emissive state also occurs in neat dendrimer films.

Figure 5 shows the PL kinetics that is detected at 600 nm in neat Ir-G1 and $Ir(ppy)_3$ films for different excitation wavelengths. The general shape and time scales of the decays are similar for different excitation wavelengths, which, together with insensitivity of the time-integrated PL spectra to the excitation wavelength (see Figure 3), indicates that the luminescence quenching in neat films is due to energy transfer to weakly emissive sites, which we refer to as quenchers. In Ir-G1 film, the PL decay is slightly slower for the long-wavelength excitation, which can be explained by slower energy transfer from the selectively excited sites of low optical gap in heterogeneous film (thus, slower quenching).

Figure 6 shows the time-resolved PL spectra for spin-coated Ir-G1 and Ir-G2 dendrimer films. The PL spectrum in Ir-G1 film at short time delays ($<0.5\ \mu$s) shows a maximum at ~515 nm and resembles the shape of the time-integrated PL spectra in solution and the blend (see Figure 3), implying that this emission comes from the same type of excited species. At 1 μs, the PL spectrum is broader and red-shifted, with respect to the early time spectrum; therefore, it is dominated by a different excited species, which does not appear in blend and solution emission. This type of behavior is expected when excitation is transferred to sites with a lower optical gap in the neat film. The spectrum does not change further on the microsecond time scale. The PL spectrum of the Ir-G2 film remains solution-like for at least 1 μs and only at ~2 μs does the shoulder appear at ~540 nm, which indicates the overlapping red-shifted emission, which is similar to the longer-time spectrum of the Ir-G1 film. Taken together, time-resolved PL spectra prove that the dominant decay components of 0.4 and 0.9 μs in dendrimer films are predominantly from the main emitting state, which has the same nature in neat film, in solution, and in the blend.

The fast components of the PL decays of the film are due to the transfer of excitations to the quenching sites. Assuming that the rates of the radiative and the direct nonradiative T_1-S_0

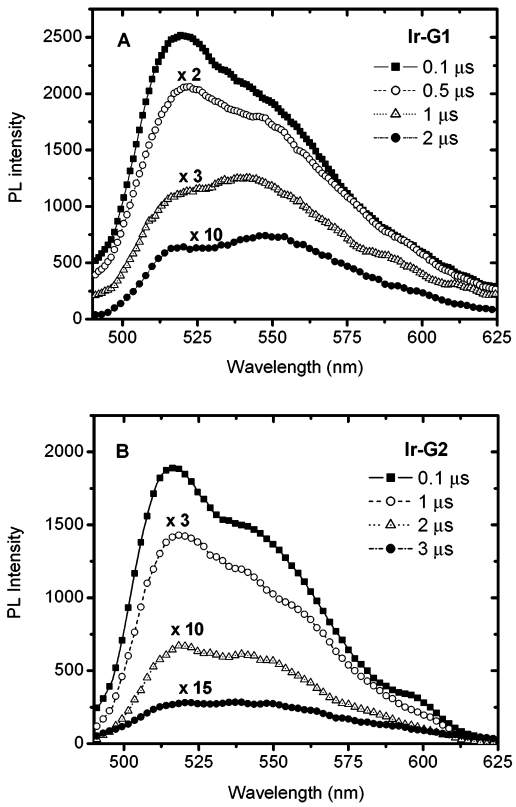

Figure 6. Time-resolved PL spectra of spin-coated (A) Ir-G1 and (B) Ir-G2 films measured after excitation at 400 nm.

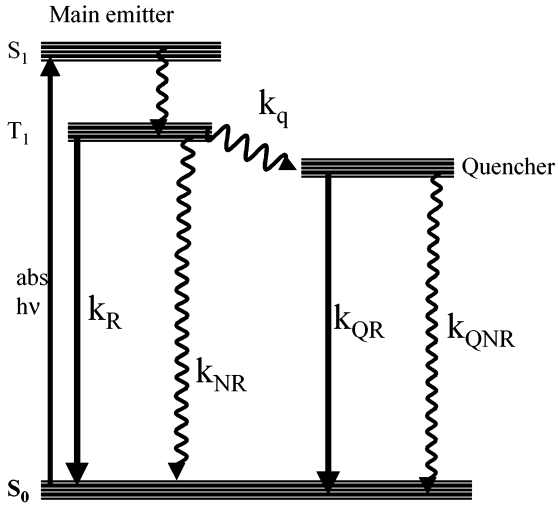

Figure 7. Kinetic model of excitation energy transfer in neat film: k_R and k_{NR} are the radiative and nonradiative decay rates of the main emitter, respectively; k_q is the energy transfer rate to the quencher; and k_{QR} and k_{QNR} are the radiative and nonradiative decay rates of the quencher, respectively.

deactivation channel in neat films are similar to those found in blends, $k_R + k_{NR} = 1/\tau_{Ph}$, then the excitation transfer rate to the quenching sites in films (Figure 7) is given by

$$k_q = \frac{1}{\tau_M} - \frac{1}{\tau_{Ph}} \tag{3}$$

where τ_M is the PL lifetime of the main emitter and $\tau_{Ph} = 1.2$ μs is the PL lifetime measured in dendrimer blends with CBP (see Table 1). For neat $Ir(ppy)_3$ films, the decay components of $\tau \approx 0.04$ μs (0.38) and $\tau \approx 0.16$ μs (0.58) observed at 550 nm give an average value $\tau_M \approx 0.1$ μs, and from eq 3, we obtain

$k_q \approx 9.2 \times 10^6\ s^{-1}$. The intensity of the red-shifted PL spectrum at 1 μs in Ir-G1 film reaches ~10% of the PL intensity at 0.1 μs, which indicates that the major fraction of the 0.9 μs component (~80%) corresponds to the main emitter. The PL decay components at 550 nm of $\tau \approx 0.08$ μs (0.02), $\tau \approx 0.4$ μs (0.44), and $\tau \approx 0.9$ μs (0.43) then give an average lifetime of $\tau_M \approx 0.6$ μs. Assuming that the natural radiative lifetime of the main emitter in the neat films is the same as that found in the blend and in solution ($\tau_R = 1.5$ μs, from eq 2), we would expect a PLQY value of ~0.40 in Ir-G1 neat film, which is higher than the value of 0.21 that is measured in the integrating sphere. A possible explanation is that some residual oxygen may have been present in the films that were used for PLQY measurements. From eq 3, we obtain $k_q \approx 0.8 \times 10^6\ s^{-1}$ for the neat Ir-G1 films. For Ir-G2 film, the PL decay components of $\tau \approx 0.3$ μs (0.14) and $\tau \approx 0.9$ μs (0.86) clearly represent the main emitter, which then has an average lifetime of $\tau_M \approx 0.76$ μs and allows the estimate of PLQY (~0.51) and k_q ($\sim 0.5 \times 10^6\ s^{-1}$). Summarizing, the excitation transfer rate to the quenching sites in films of Ir-G1 and Ir-G2 is slower than that in neat $Ir(ppy)_3$ film by a factor of ~11 and ~20, respectively. One can note that these rates are rather slow, in comparison to the typical triplet−triplet nearest-neighbor transfer rates of 10^8−$10^9\ s^{-1}$ that have been observed (for instance, in anthracene crystals[22]), which indicates that extensive migration is involved until excitations are captured by quenchers. This observation shows that the concentration of the quenchers is low.

Our results do not provide conclusive evidence about the nature of the PL quenchers. According to calculations, the highest occupied molecular orbitals (HOMOs) in $Ir(ppy)_3$ are mixtures of Ir^{3+} orbitals and π orbitals of the ligand, whereas the lowest unoccupied molecular orbitals (LUMOs) are combinations of π^* orbitals of the ligands.[18,19] It is sensible to expect that intermolecular interactions in $Ir(ppy)_3$ are mainly determined by π and π^* orbitals of the ligands; therefore, the interactions are likely to increase when one of neighboring molecules is in an excited state, and, thus, intermolecular excimer states are likely to form in $Ir(ppy)_3$ films at the sites where intermolecular orientation is favorable for close packing of the ligands. When excitation is transferred to one of these sites during migration, its energy is reduced by the interaction energy and these sites act as excitation traps. The nonradiative decay channel usually prevails in excimers; therefore, they would act as weakly emissive luminescence quenchers. Other possibilities could be a weakly emissive isomer or impurity that is present at low concentration.

D. Film Morphology. We observe evidence for the formation of aggregates or microdomains from surface morphology measurements of the films using atomic force microscopy (AFM). Figure 8 shows the AFM images of a 110-nm-thick spin-coated film of Ir-G1 and an evaporated 100-nm-thick Ir-$(ppy)_3$ film on quartz substrates. The surface of the dendrimer film (the root-mean-square (RMS) roughness of which is ~1 nm) is much smoother than that of the $Ir(ppy)_3$ film (RMS roughness of ~4 nm). RMS values of ~1 nm are also observed for Ir-G2 and (Ir-G1):CBP blends. The evaporated film has rodlike structures, which indicate aggregation in the films. We note that the rodlike (or needle-shaped) structures are bigger than the actual size of the aggregates; however, they are the regions of the sample where the aggregates are most likely to form. Interestingly, needle-shaped aggregates were recently reported by Noh et al.[21] in a blend of $Ir(ppy)_3$ (15 wt %) in poly[9,9′-di-*n*-hexyl-2,7-fluorene-*alt*-1,4-(2,5-di-*n*-hexyloxy)-phenylene]. This suggests that $Ir(ppy)_3$ can also aggregate in blends, which is consistent with the presence of the fast-decay component in the 7% $Ir(ppy)_3$ blend with CBP (see Figure 4A and Table 1). In contrast, the spin-coated dendrimer films were homogeneous, with no phase separation or rodlike structures, which suggests that the dendritic structures discourage aggregation and form homogeneous films.

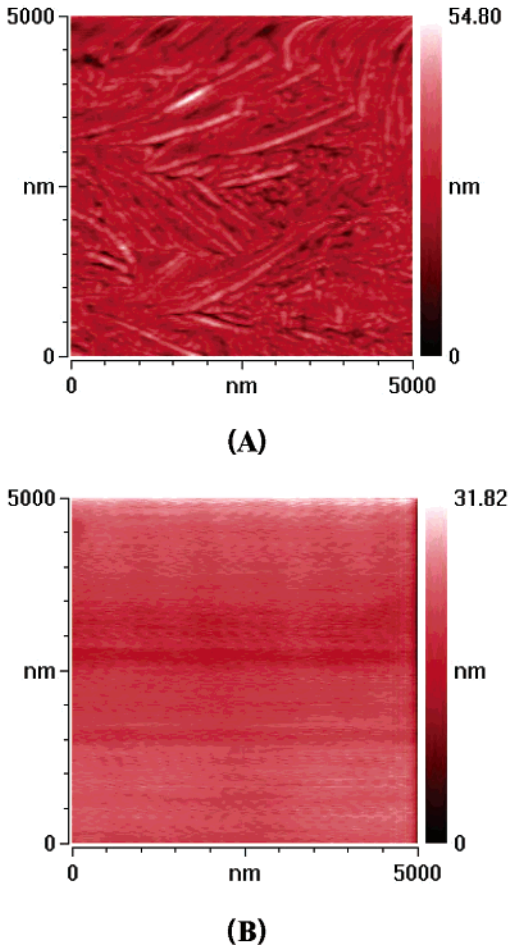

Figure 8. AFM images of (A) an evaporated 100-nm-thick $Ir(ppy)_3$ film and (B) a spin-coated 110-nm-thick Ir-G1 film.

E. Radiative Lifetime of the Quencher in $Ir(ppy)_3$ Films. The amplitude of the 0.9-μs decay component in $Ir(ppy)_3$ films increases substantially as the emission wavelength increases (see Table 2), which suggests the presence of a long-life red-shifted emitter. Obviously, it is responsible for the apparent red shift of the time-integrated PL spectrum in this film, with respect to the blend and solution, so we attribute the long-decay component of 0.9 μs in $Ir(ppy)_3$ films to the quencher. If light emission comes from two species (the main emitter and the quencher), then the measured PLQY value in the film is a sum of their contributions:

$$\mathrm{PLQY} = \Phi_M + \Phi_Q \tag{4}$$

$$\Phi_M = \frac{G_M \tau_M}{\tau_R} \tag{5}$$

and

$$\Phi_Q = \frac{G_Q \tau_Q}{\tau_{QR}} \tag{6}$$

where G_M and G_Q are population efficiencies of the main emitter and the quencher, respectively. The parameters τ_M and τ_Q are

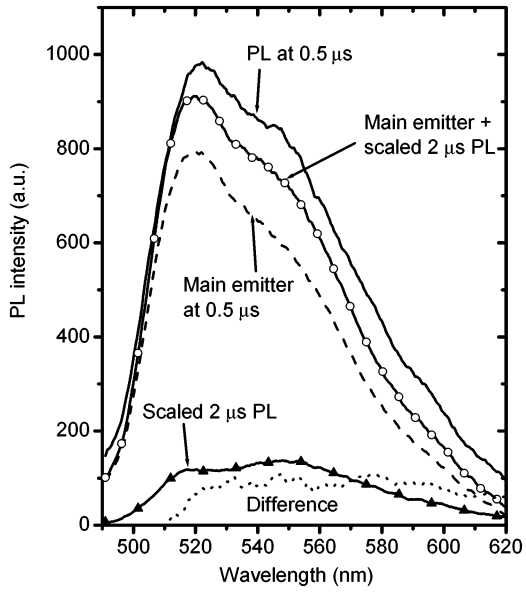

Figure 9. PL spectrum of neat Ir-G1 film at 0.5 μs (solid line) and the reconstructed spectrum (open circles) taken as a sum of the main emitter (dashed line) and the scaled 2-μs spectrum using eq 9 (triangles). Dotted line represents the difference between the measured and reconstructed spectra at 0.5 μs.

the respective lifetimes of the main emitter and the quencher, whereas τ_R and τ_{QR} are the respective radiative lifetimes.

From the photophysical model in Figure 7, assuming that all excitations that did not emit and have not decayed nonradiatively are trapped by quenchers, we obtain

$$G_Q = \frac{k_q}{k_R + k_{NR} + k_q} = k_q \tau_M \qquad (7)$$

For neat Ir(ppy)$_3$ films, if $\tau_M \approx 0.1$ μs, $\tau_R = 1.5$ μs, and G_M is assumed to be unity, then $\Phi_M = 0.07$. The PL decays in Ir(ppy)$_3$ films were similar when measured under vacuum and under flowing nitrogen; thus, $\Phi_Q = 0.12 - \Phi_M \approx 0.05$, $k_q \approx 9.2 \times 10^6$ s^{-1}, and $G_Q \approx 0.92$. The PL decay component of $\sim$0.9 μs is assigned to the quencher emission; thus, $\tau_Q = 0.9$ μs. From eq 6, we then get $\tau_{QR} \approx 17$ μs, which is an order of magnitude longer than the radiative lifetime of the main emitter ($\tau_R = 1.5$ μs). This shows that PL quenchers in neat Ir(ppy)$_3$ films possess an oscillator strength that is an order of magnitude weaker than that of the main emitter and suggests they may be excimers or dimers. We note that the decrease of the oscillator strength, by an order of magnitude, has also been observed in the interchain aggregates of fluorescent conjugated polymers.[23,24]

F. Evidence for Two Types of Emitting Species in Dendrimer Film. In the aforementioned model, there are two emitting species; therefore, we should be able to reconstruct the PL spectra at intermediate time delays by a superposition of the corresponding spectra of the main emitter and quencher:

$$I(t) = I_M(t) + I_Q(t) \qquad (8)$$

For the PL spectrum of the main emitter, we can use the spectrum taken at 0.1 μs, by scaling it by the measured PL kinetics (see Figure 4). For the neat Ir-G1 film, $I_M(0.5\ \mu s) = 0.45 \times I(0.1\ \mu s)$. For a moment, we assume that the emission of the quencher in Ir-G1 film could be represented by the PL spectrum at a time delay of 2 μs. The population of the quenchers can be described as the multiplication of the rise term with the rate constants k_{qi} and pre-exponential factors A_i, and the decay term with a time constant τ_Q; thus,

$$I_Q(t) \approx I(2\ \mu s) \times [1 - \sum_{i=1}^{3} A_i \exp(-k_{qi} t)] \times \exp\left(-\frac{t(\mu s) - 2}{\tau_Q}\right) \qquad (9)$$

where $k_{qi} = (1/\tau_i) - (1/\tau_{Ph})$; τ_i and A_i respectively are time constants and pre-exponential factors in the three-exponential decay fits (see Table 2); and $\tau_{Ph} = 1.2$ μs. For the neat Ir-G1 film, $\tau_Q \approx 0.9$ μs. Figure 9 illustrates that the intensity of the reconstructed spectrum at $t = 0.5$ μs is lower in the spectral range of 510−620 nm than the measured 0.5-μs spectrum. This difference comes from the fact that the decay term in eq 9 does not consider the delay in the formation of the quencher population and, thus, it overestimates the decay of the quencher emission. The intensity difference between the measured and the reconstructed 0.5-μs spectra therefore represents the pure PL spectrum of the quencher, whereas the 2-μs spectrum contains the contribution from the main emitter, which shows an apparent shoulder at $\sim$520 nm.

4. Conclusions

Through the combination of time-resolved photoluminescence (PL) and photoluminescence quantum yield (PLQY) measurements, we have determined the time constants of the natural radiative (τ_R) and nonradiative (τ_{NR}) deactivation of the lowest excited state in the Ir(ppy)$_3$ molecule, as well as those in the first- and second-generation Ir(ppy)$_3$ cored dendrimers. The molecular Ir(ppy)$_3$ and dendrimers show very similar values of τ_R (1.5 ± 0.2 μs) and τ_{NR} (6 ± 1 μs), which indicates that the addition of the dendrons to Ir(ppy)$_3$ does not change the luminescence properties of the individual molecules. In neat films, the PL lifetime was observed to be much longer for dendrimers than for the molecular Ir(ppy)$_3$, which is consistent with higher PLQY values that have been measured for dendrimer films. We have shown that PL quenching in neat films occurs because of energy transfer to less-emissive sites (quenchers), and the effective rate of energy transfer to the quenchers in neat films (k_q) is $\sim 9.2 \times 10^6$ s^{-1} for Ir(ppy)$_3$, $\sim 0.8 \times 10^6$ s^{-1} for Ir-G1, and $\sim 0.5 \times 10^6$ s^{-1} for Ir-G2. Extensive aggregation of Ir(ppy)$_3$ molecules is indicated by their rough surface with aggregated regions of rodlike structure, as obtained by atomic force microscopy, which suggests that the PL quenchers in neat Ir(ppy)$_3$ films may be excimers. Dendritic structures reduce the PL quenching rate and provide a powerful and systematic way of controlling intermolecular interactions in films. This observation is supported by the much smoother surface of dendrimer films than that of Ir(ppy)$_3$ films.

Acknowledgment. The authors wish to thank CDT Oxford, Ltd., as well as EPSRC and SHEFC, for financial assistance. I.D.W.S. is a Royal Society Research Fellow.

References and Notes

(1) Tang, C. W.; Van Slyke, S. A. *Appl. Phys. Lett.* **1987**, *51*, 913.
(2) Friend, R. H.; Gymer, R. W.; Holmes, A. B.; Burroughes, J. H.; Marks, R. N.; Tallani, C.; Bradley, D. D. C.; Dos Santos, D. A.; Brédas, J. L.; Lögdlund, M.; Salaneck, W. R. *Nature* **1999**, *397*, 121.
(3) Burroughes, J. H.; Bradley, D. D. C.; Brown, A. R.; Marks, R. N.; Mackay, K.; Friend, R. H.; Burn, P. L.; Holmes, A. B. *Nature* **1990**, *347*, 539.

(4) Cao, Y.; Parker, I. D.; Yu, G.; Zhang, C.; Heeger, A. *Nature* **1999**, *397*, 414.
(5) Markham, J. P. J.; Lo, S.-C.; Magennis, S. W.; Burn, P. L.; Samuel, I. D. W. *Appl. Phys. Lett.* **2002**, *80*, 2645.
(6) Lo, S.-C.; Male, N. A. H.; Markham, J. P. J.; Magennis, S. W.; Burn, P. L.; Salata, O. V.; Samuel, I. D. W. *Adv. Mater.* **2002**, *14*, 975.
(7) Pillow, J. N. G.; Halim, M.; Lupton, J. M.; Burn, P. L.; Samuel, I. D. W. *Macromolecules* **1999**, *32*, 5985.
(8) Halim, M.; Pillow, J. N. G.; Samuel, I. D. W.; Burn, P. L. *Adv. Mater.* **1999**, *11*, 371.
(9) Webber, P. W.; Liu, Y. J.; Devadoss, C.; Bharathi, P.; Moore, J. S. *Adv. Mater.* **1996**, *8*, 237.
(10) Freeman, A. W.; Shannon, C. K.; Malenfant, P. R. L.; Thompson, M. E.; Fréchet, J. M. J. *J. Am. Chem. Soc.* **2000**, *122*, 12385.
(11) Baldo, M. A.; Thomson, M. E.; Forrest, S. R. *Nature* **2000**, *403*, 750.
(12) Kolosov, D.; Adamovich, V.; Djurovich, P.; Thompson, M. E.; Adachi, C. *J. Am. Chem. Soc*. **2002**, *124*, 9945.
(13) Das, R. R.; Lee, C.-L.; Kim, J. J. *Mater. Res. Soc. Symp. Proc.* **2002**, BB3.39.1.
(14) Sprouse, S.; King, K. A.; Spellane, P. J.; Watts, R. J. *J. Am. Chem. Soc.* **1984**, *106*, 6647.
(15) Wang, Y.; Herron, N.; Grushin, V. V.; LeCloux, D.; Petrov, V. *Appl. Phys. Lett*. **2001**, *79*, 449.
(16) Demas, J. N.; Crosby, G. A. *J. Phys. Chem.* **1971**, *75*, 991.
(17) Greenham, N. C.; Samuel, I. D. W.; Hayes, G. R.; Phillips, R. T.; Kessener, R. R.; Moratti, S. C.; Holmes, A. B. *Chem. Phys. Lett*. **1995**, *241*, 89.
(18) Hay, P. J. *J. Phys. Chem. A* **2002**, *106*, 1634.
(19) Tamayo, A. B.; Alleyne, B. D.; Djurovich, P.; Lamansky, S.; Tsyba, I.; Ho, N. N.; Bau, R.; Thompson, M. E. *J. Am. Chem. Soc*. **2003**, *125*, 7377.
(20) Adachi, C.; Baldo, M. C.; Forrest, S. R.; Thompson, M. E. *Appl. Phys. Lett*. **2000**, *77*, 904.
(21) Noh, Y.-Y.; Lee, C.-L.; Kim, J.-J.; Yase, K. *J. Chem. Phys.* **2003**, *118*, 2853.
(22) Ern, V.; Bouchriha, H.; Schott, M.; Castro, G. *Chem. Phys. Lett*. **1974**, *29*, 453.
(23) Samuel, I. D. W.; Rumbles, G.; Collison, C. J. *Phys. Rev. B* **1995**, *52*, R11573.
(24) Ruseckas, A.; Namdas, E. B.; Theander, M.; Svensson, M.; Yartsev, A.; Zigmantas, D.; Andersson, M. R.; Inganäs, O.; Sundström, V. *J. Photochem. Photobiol. A* **2001**, *5810*, 1.